

Article

Theory for Electrochemical Heat Sources and Exothermic Explosions: The Akbari–Ganji Method

Ramalingam Vanaja ¹, Ponraj Jeyabarathi ², Lakshmanan Rajendran ^{1,*}  and Michael Edward Gerard Lyons ^{3,*} ¹ Department of Mathematics, AMET, Deemed to Be University, Chennai 625003, India² Department of Mathematics, Bharath Institute of Higher Education and Research, Chennai 600073, India; bsc.jeya@yahoo.com³ School of Chemistry, AMBER National Centre, University of Dublin, Trinity College Dublin, D02 PN 40 Dublin, Ireland

* Correspondence: raj_sms@rediffmail.com (L.R.); melyons@tcd.ie (M.E.G.L.)

Abstract: A device that transforms chemical energy into electrical energy is an electrochemical cell. The reaction type inside the cell determines whether it is exothermic or endothermic. This paper discusses the mathematical modelling of exothermic explosions in a slab. This model is based on a nonlinear equation containing a nonlinear term related to Arrhenius, bimolecular, and sensitised laws of reaction kinetics. The absolute temperature can be derived by solving the nonlinear equation using the Akbari–Ganji technique. The mathematical model also numerically solved and simulated in the MATLAB® v2016b software. The new simple theoretical result is validated with previously identified analytical and numerical findings. The influence of the parameters of Frank-Kamenetskii number, activation energy and the numerical exponent on temperature is discussed. The Frank-Kamenetskii number is observed to drop as the temperature is found to decrease, while the activation energy parameter is shown to increase. The numerical exponent has little or no effect on the temperature. An extension of this model to cylinder and sphere geometry is also provided.

Keywords: electrochemical heat sources; exothermic explosions; mathematical modelling; nonlinear equation; Akbari–Ganji method



Citation: Vanaja, R.; Jeyabarathi, P.; Rajendran, L.; Lyons, M.E.G. Theory for Electrochemical Heat Sources and Exothermic Explosions: The Akbari–Ganji Method. *Electrochem* **2023**, *4*, 424–434. <https://doi.org/10.3390/electrochem4030027>

Academic Editor: Masato Sone

Received: 26 June 2023

Revised: 21 August 2023

Accepted: 24 August 2023

Published: 5 September 2023



Copyright: © 2023 by the authors. Licensee MDPI, Basel, Switzerland. This article is an open access article distributed under the terms and conditions of the Creative Commons Attribution (CC BY) license (<https://creativecommons.org/licenses/by/4.0/>).

1. Introduction

Numerous industries, such as heavy oil recovery, the storage of cellulosic compounds, coal gasification, waste burning, biomass and coal combustion, and lithium-ion batteries, have researched the thermal breakdown of reactive materials due to exothermic chemical reactions. Thus, it is highly desirable to model the situation mathematically. Many researchers have provided models to explain abusive behaviour and thermal runaway. Hatchard et al. [1] took the initial steps to explain the exothermic reaction kinetics in prismatic and cylindrical lithium-ion cells. Furthermore, they accurately predicted the variation in cell temperature during and after nail penetration using a numerical simulation. A modified reaction–diffusion theory was provided in the works of Kim et al. [2] and Peng et al. [3,4]. An electrochemical model of lithium-ion battery nail penetration, which involved a dramatic temperature change, was also discussed in [5]. A catastrophe theory approach based on a simplified ordinary differential equation has also been reported [6]. This model was extended in [7,8].

Ziebert et al. [9] discussed electrochemical–thermal characterization and thermal modelling for batteries. Guo et al. [10] developed the three-dimensional thermal finite element modelling of lithium-ion batteries in thermal abuse applications. In 1930, Semonov, Zeldovith, and Frank-Kamenetskii described this behaviour first, and their pioneering contributions were presented in [11]. Frank-Kamenetskii also proposed the steady-state theory of thermal explosions. This idea has been applied to various combustible material geometries in the literature. For an infinite slab, Boddington et al. [12–14] and Wake

et al. [15] reviewed a case of two-step parallel exothermic processes, and they extended the investigations to two other geometries of an infinite circular cylinder and a sphere. Balakrishnan et al. [16] obtained critical values for some geometries, such as infinite squares, rods, and cubes, using the finite difference method.

Makinde et al. [17] obtained analytical solutions for the governing nonlinear boundary value problem using the perturbation technique and Hermite–Pade approximants. Also, they discussed the essential properties of a temperature field, including bifurcations and thermal criticality. Ananthasamy et al. [18] used the homotopy analysis method to solve a nonlinear equation to obtain an analytical expression of the temperature in an exothermic explosion in a slab. This is time-consuming since it contains an infinite number of convergence control parameters. Er-Riani and Chetehouna [19] applied the homotopy perturbation method to solve the steady-state nonlinear equation in an exothermic chemical reaction. This perturbation method has a convergence problem, however, and requires a small parameter. In this paper, we obtain a simple analytical expression for the temperature field for a range of kinetic mechanisms, such as sensitised, Arrhenius, and bimolecular reactions, by solving the nonlinear Frank-Kamenetskii equation using the very useful Akbari–Ganji method.

2. Mathematical Formulation and Analysis of the Problems

Considering the steady state of an exothermic chemical reaction in a combustible slab with the potential of heat loss to the environment, Frank-Kamenetskii [11] first proposed the classical formulation of this problem. The heat balance equation for steady-state conditions is given as follows [19]:

$$k \frac{d^2 T(Y)}{d Y^2} + Q C_0 A \left(\frac{K T(Y)}{v h} \right)^m e^{\frac{-E}{R T(Y)}} = 0 \quad (1)$$

The boundary conditions are

$$\frac{d T}{d Y} = 0 \text{ at } Y = 0, \quad (2)$$

$$T = T_0 \text{ at } Y = a, \quad (3)$$

where T denotes the absolute temperature, k represents the material's thermal conductivity, Q is the heat of the reaction, C_0 is the initial concentration of the reactant species, A is the rate constant, h indicates Planck's number, v denotes the vibration frequency, K is Boltzmann's constant, E represents the activation energy, R is the universal gas constant, a is the slab half width, Y is the distance measured in the normal direction in the plate, and T_0 is the wall temperature. The parameter m is the numerical constant, so that $m = 2, 0, 1/2$ indicates the numerical exponent for sensitised, Arrhenius, and bimolecular kinetics. To reduce the complexity, we make the nonlinear Equation (1) into a dimensionless form by defining the following dimensionless parameters:

$$\theta = \frac{E(T - T_0)}{R T_0^2}, \quad \varepsilon = \frac{R T_0}{E}, \quad y = \frac{Y}{a}, \quad \lambda = \frac{Q E A a^2 C_0 K^m T_0^{m-2} e^{\frac{E}{R T_0}}}{v^m h^m R k} \quad (4)$$

where θ is the dimensionless temperature field, λ denotes the Frank-Kamenetskii parameter, ε represents the activation energy parameter, and y is the dimensionless distance. If the Frank-Kamenetskii parameter λ is greater than a critical value, an explosion occurs and the differential equation does not have a solution. Using Equation (4), Equation (1) reduces this to the following dimensionless form:

$$\frac{d^2 \theta(y)}{d y^2} + \lambda (1 + \varepsilon \theta(y))^m e^{\left(\frac{\theta(y)}{1 + \varepsilon \theta(y)} \right)} = 0 \quad (5)$$

The dimensionless boundary conditions are

$$\frac{d\theta}{dy} = 0 \text{ at } y = 0, \quad (6)$$

$$\theta = 0 \text{ at } y = 1, \quad (7)$$

3. New Analytical Expression of the Temperature Distribution Using the Akbari–Ganji Method

The Taylor series [20,21], Adomian decomposition [22], variational iteration [23], and Akbari–Ganji methods [24] are only a few of the asymptotic techniques that have been applied to solve nonlinear differential equations. Among these techniques, the AGM (discussed in Appendix A) might be regarded as a useful algebraic (semi-analytic) approach to resolving such issues. According to the AGM, a solution function with unidentified constant coefficients is supposed to satisfy the differential equation and the initial conditions. We can assume that the trial solution of Equation (5) is

$$\theta(y) = \sum_{i=0}^2 \theta_i y^i = \theta_0 + \theta_1 y + \theta_2 y^2 \quad (8)$$

where θ_0 , θ_1 , and θ_2 are constants. Using the boundary conditions (6) and (7), we obtain

$$\theta_1 = 0, \quad \theta_0 = -\theta_2 \quad (9)$$

Now, we can define the function G by

$$G(y) = \frac{d^2\theta}{dy^2} + \lambda(1 + \varepsilon\theta)^m e^{\left(\frac{\theta}{1+\varepsilon\theta}\right)} = 0 \quad (10)$$

Using Equation (8), Equation (10) at $y = 0$ becomes

$$G(y = 0) = 2\theta_2 + \lambda(1 - \varepsilon\theta_2)^m e^{\left(\frac{-\theta_2}{1-\varepsilon\theta_2}\right)} = 0 \quad (11)$$

Using Equation (9), Equation (8) can be rewritten as follows:

$$\theta(y) = \theta_2(y^2 - 1) \quad (12)$$

The parameter θ_2 is obtained by solving the nonlinear Equation (13).

$$2\theta_2 + \lambda(1 - \varepsilon\theta_2)^m e^{\left(\frac{-\theta_2}{1-\varepsilon\theta_2}\right)} = 0 \quad (13)$$

The unknown parameter θ_2 can be obtained by solving Equation (13) using Matlab R2019b or Wolfram [Alpha.com](https://www.wolfram.com) (free online software, accessed on 4 September 2023).

4. Previous Analytical Results

The homotopy analysis method and the perturbation methodology may both be utilised to solve the nonlinear Equation (5) efficiently, as suggested by Anathaswamy's work [18] and Makinde et al.'s study [17]. The lengthy expressions obtained in the aforementioned publications may cause some convergence issues for inexperienced users. Therefore, we tackle the problem directly in our paper using the AGM method which has been found effective for analysing transport and kinetics in bounded regions [24,25]. This methodology provided approximate closed form expressions for the temperature distribution in the region, which is in good agreement with numerical simulations.

5. Discussion

Equation (12) represents the simplest analytical expression of the temperature profile. The thermal decomposition of the reacting combustible material depends on the parameters λ , ε and m , which are of great importance to applications in industrial safety and the handling techniques of explosives.

Numerical Simulation

This section validates the above theoretical results using a numerical simulation for physically realistic values of various embedded parameters. The function `bvp4c` in Matlab/Scilab software (Version 9.11), which solves nonlinear boundary value problems for ordinary differential equations, is used to solve these equations numerically. The present (AGM) and previous (HAM, PM) analytical results are compared to this numerical solution in Tables 1–4. The maximum average relative error between our result and the simulation result is 1.44%. But the maximum error between numerical results and HAM and PM is 1.86% and 4.92%, respectively. In the computations, we solve the Frank-Kamenetskii equation for the kinetic cases where $m = -2$ and $m = 0$ corresponding to sensitised and Arrhenius kinetics.

Table 1. Comparison of dimensionless temperature field $\theta(y)$ with simulation results and previous analytical results for $\lambda = 0.1$, $\varepsilon = 0.1$, $m = -2$ and $\theta_2 = -0.05175$.

y	$\theta(y)$						
	Num.	AGM Equation (12) This Work	HAM [18]	PM [17]	Error % AGM Equation (12) This Work	Error % HAM [18]	Error % PM [17]
0	0.0517	0.0517	0.0517	0.0516	0.0000	0.0000	0.1934
0.2	0.0496	0.0496	0.0496	0.0495	0.0000	0.0000	0.2016
0.4	0.0432	0.0436	0.0434	0.0433	0.9259	0.0230	0.4629
0.6	0.0327	0.0324	0.0330	0.0329	0.9174	0.0303	0.6116
0.8	0.0179	0.0180	0.0185	0.0185	0.5586	3.3519	3.3519
1	0.0000	0.0000	0.0000	0.0000	0.0000	0.0000	0.0000
Average error (%)					0.3493	0.5675	0.8036

Table 2. Comparison of dimensionless temperature field $\theta(y)$ with simulation results and previous analytical results for $\lambda = 0.5$, $\varepsilon = 0.1$, $m = -2$, and $\theta_2 = -0.320092$.

y	$\theta(y)$						
	Num.	AGM Equation (12) This Work	HAM [18]	PM [17]	Error % AGM Equation (12) This Work	Error % HAM [18]	Error % PM [17]
0	0.3045	0.3201	0.2951	0.2823	4.8133	3.0870	7.2906
0.2	0.2916	0.3001	0.2829	0.2707	2.8000	2.9835	7.1673
0.4	0.2532	0.2548	0.2466	0.2363	0.6319	2.5671	6.6745
0.6	0.1899	0.1893	0.1869	0.1792	0.3159	1.5798	5.6334
0.8	0.1031	0.1030	0.1041	0.1002	0.0970	0.9699	2.8128
1	0.0000	0.0000	0.0000	0.0000	0.0000	0.0000	0.0000
Average error (%)					1.4430	1.8645	4.9298

Table 3. Comparison of dimensionless temperature field $\theta(y)$ with simulation results and previous analytical results for $\lambda = 0.1$ when $\varepsilon = 0.1$, $m = 0$, $\theta_2 = -0.0523$.

y	$\theta(y)$						
	Num.	AGM Equation (12) This Work	HAM [18]	PM [17]	Error % AGM Equation (12) This Work	Error % HAM [18]	Error % PM [17]
0	0.0522	0.0523	0.0521	0.0522	0.1916	0.1916	0.0000
0.2	0.0501	0.0501	0.0500	0.0501	0.0000	0.1996	0.0000
0.4	0.0436	0.0437	0.0437	0.0438	0.2294	0.2294	0.4587
0.6	0.0329	0.0331	0.0332	0.0333	0.6079	0.9118	1.2158
0.8	0.0180	0.0181	0.0188	0.0187	0.5555	4.4444	3.8889
1	0.0000	0.0000	0.0000	0.0000	0.0000	0.0000	0.0000
Average error (%)					0.2641	0.9961	0.9272

Table 4. Comparison of dimensionless temperature field $\theta(y)$ with simulation results and previous analytical results for $\lambda = 0.4$, $\varepsilon = 0.1$, $m = 0$, $\theta_2 = -0.32181$.

y	$\theta(y)$						
	Num.	AGM Equation (12) This Work	HAM [18]	PM [17]	Error % AGM Equation (12)	Error % HAM [18]	Error % PM [17]
0	0.3255	0.3208	0.3192	0.3172	1.4439	1.9355	2.5499
0.2	0.3116	0.3077	0.3059	0.3040	1.2516	1.8292	2.4390
0.4	0.2701	0.2684	0.2662	0.2646	0.6294	1.4439	2.0363
0.6	0.2021	0.2030	0.2011	0.1994	0.4433	0.4948	1.3360
0.8	0.1093	0.1113	0.1117	0.1110	1.8230	2.1958	1.5553
1	0.0000	0.0000	0.0000	0.0000	0.0000	0.0000	0.0000
Average error (%)					0.9319	1.3163	1.6527

6. Limiting Case

We now examine the general expression presented in Equation (5) and look at the case when the activation energy parameter is small so $\varepsilon\theta \ll 1$. Under such circumstances, Equation (5) becomes

$$\frac{d^2\theta}{dy^2} + \lambda e^\theta = 0 \tag{14}$$

In this case, the temperature profile becomes

$$\theta(y) = \log \left[\frac{n - n \operatorname{Tanh}^2(0.5y \sqrt{n})}{2\lambda} \right] \tag{15}$$

where n is obtained from the equation

$$n - n \operatorname{Tanh}^2(0.5\sqrt{n}) = 2\lambda \tag{16}$$

In Table 5, we compare the approximate analytical result obtained using the AGM presented in Equation (12), with the analytical solution outlined in Equation (15) for the limiting case when $\varepsilon\theta \ll 1$. We can notice that the average error percentage between the AGM and an exact limiting case result (Equation (15)) did not exceed 1.8% for the slab geometry. This is an indication of the usefulness of the AGM.

Table 5. Comparison of our approximate analytical result (12) with the exact result (19) for the limiting case.

y	$\lambda=0.1$			$\lambda=0.3$			$\lambda=0.5$		
	Exact Solution Equation (15)	AGM Equation (12)	Error %	Exact Solution Equation (15)	AGM Equation (12)	Error %	Exact Solution Equation (15)	AGM Equation (12)	Error %
0	0.0522	0.0527	0.9578	0.1733	0.1795	3.5776	0.3290	0.3474	5.5927
0.2	0.0501	0.0505	0.7984	0.1661	0.1689	1.6857	0.3148	0.3246	3.1131
0.4	0.0436	0.0439	0.6881	0.1443	0.1440	0.2079	0.2728	0.2768	1.4663
0.6	0.0329	0.0330	0.3039	0.1085	0.1087	0.1843	0.2040	0.2060	0.9804
0.8	0.0180	0.0180	0.0000	0.0590	0.0590	0.0000	0.1102	0.1102	0.0000
1	0.0000	0.0000	0.0000	0.0000	0.0000	0.0000	0.0000	0.0000	0.0000
	Average error (%)		0.4580	Average error (%)		0.9426	Average error (%)		1.8587

7. Influence of the Parameters on Temperature

7.1. Influence of the Frank-Kamenetskii Parameter λ on Temperature

Figure 1 illustrates the effects of the Frank-Kamenetskii parameter on a temperature profile for the various reaction mechanisms. From the figure, it is observed that the rate of an exothermic reaction increased with the increase in the Frank-Kamenetskii parameter. The slab internal heat generation caused by the exothermic reaction increased as the Frank-Kamenetskii parameter increased. The slab temperature invariably rises as a result of this.

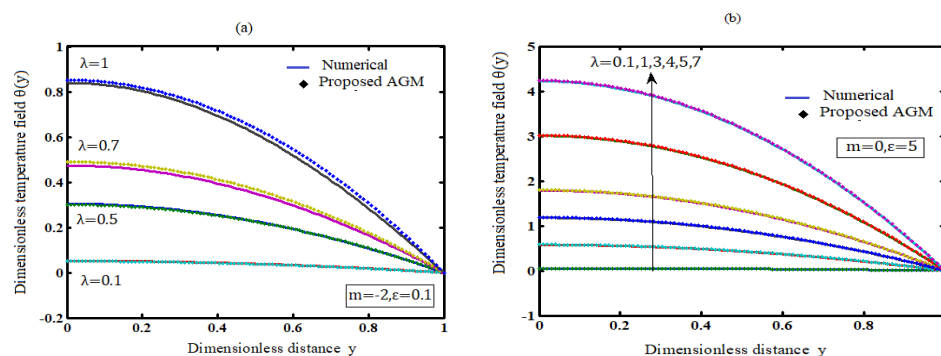


Figure 1. Comparison of analytical expression of temperature field $\theta(y)$ with simulation results for different values of Frank-Kamenetskii parameter (λ) using Equation (12). The sub-figures indicate the temperature profiles computed for (a) sensitised ($m = -2$), and (b) Arrhenius ($m = 0$) kinetics for two specified values of normalised inverse activation energy ε .

7.2. Influence of the Numerical Exponent (m) on Temperature

The effects of the numerical exponent m , defining the type of reaction kinetics, on the temperature profiles are shown in Figure 2a. The figure shows that the temperature increased as the numerical exponent number m increased. Moreover, the tables and figures show that in the bimolecular ($m = 0.5$) type of exothermic reaction, a thermal explosion occurred faster than in the Arrhenius ($m = 0$) and sensitised ($m = -2$) reactions.

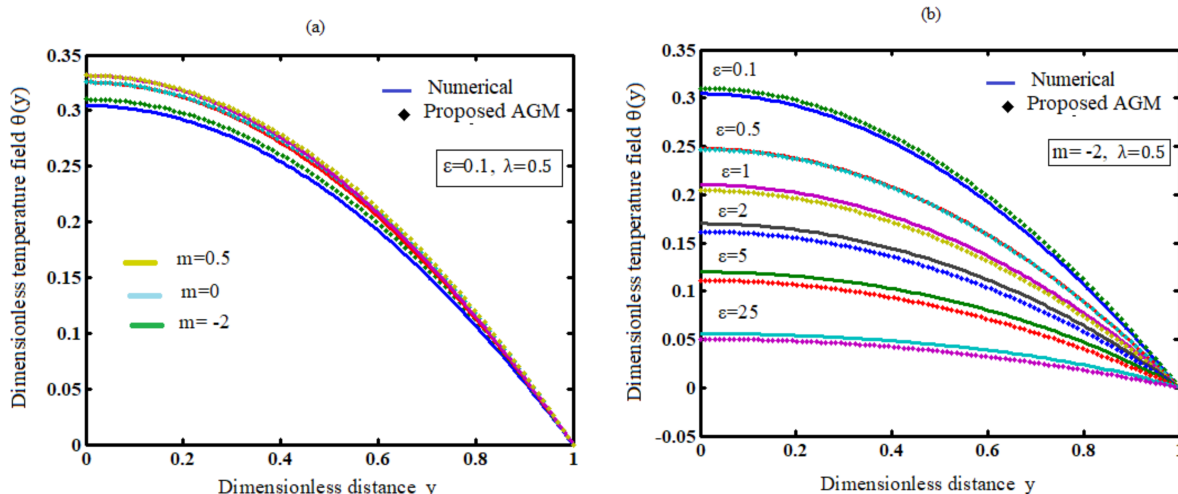


Figure 2. Comparison of temperature field $\theta(y)$ with simulation results (a) for various values of m (kinetics) and (b) for various values of ϵ (activation energy parameter). The numerical simulations are illustrated using blue and the analytical approximation via the AGM is illustrated using a number of other colours.

7.3. Influence of the Activation Energy Parameter (ϵ) on Temperature

A similar effect of temperature was observed with increasing values of the activation energy parameter (ϵ). The influence of the activation energy parameter on the temperature profile is shown in Figure 2b. With rising values of the activation energy parameter ϵ , a similar effect of temperature enhancement was observed. Increasing values of ϵ imply that the reacting slab’s activation energy was insufficient, and thus the reacting slab’s volatility characteristic was significantly reduced.

The overall activation energy of the process reduced as the temperature rose (Figure 2b). Faster Li ion diffusion is directly correlated with lower activation energy, which leads to higher power outputs from the electrode. Thus, our analytical result will help to develop higher-power batteries and electrode materials with faster ionic diffusion in lithium-ion cells.

7.4. Extension of the Theoretical Model for Cylindrical and Spherical Geometries

This section briefly indicates some extensions to the theoretical model outlined in this paper. The nonlinear reaction–diffusion equation for cylindrical and spherical geometries can be written as follows [19]:

$$\frac{d^2\theta}{dy^2} + \frac{j}{y} \frac{d\theta}{dy} + \lambda(1 + \epsilon \theta)^m e^{\left(\frac{\theta}{1+\epsilon \theta}\right)} = 0 \tag{17}$$

where $j = 0, 1$, and 2 represent the geometry factors for the slab, cylinder, and sphere. The dimensionless boundary conditions are

$$\theta'(0) = 0 \tag{18}$$

$$\theta(1) = 0 \tag{19}$$

We can assume that the equation’s solution has the following form:

$$\theta(y) = \sum_{i=0}^2 \theta_i y^i = \theta_0 + \theta_1 y + \theta_2 y^2 \tag{20}$$

where θ_0, θ_1 , and θ_2 are constants. Using the boundary conditions (18) and (19), we obtain

$$\theta_1 = 0, \quad \theta_0 = -\theta_2 \tag{21}$$

Now, Equation (20) becomes

$$\theta(y) = \theta_2 y^2 - \theta_2 \quad (22)$$

The function G will now be defined by

$$G(y) = \frac{d^2\theta}{dy^2} + \frac{j}{y} \frac{d\theta}{dy} + \lambda(1 + \varepsilon\theta)^m e^{\left(\frac{\theta}{1+\varepsilon\theta}\right)} = 0 \quad (23)$$

Using Equation (22), Equation (23) at $y = 0.5$ becomes

$$G(y = 0.5) = 2\theta_2(1 + j) + \lambda(1 - 0.75\theta_2\varepsilon)^m e^{\left(\frac{-0.75\theta_2}{1-0.75\theta_2\varepsilon}\right)} = 0 \quad (24)$$

Hence, the solution of Equation (17) is

$$\theta(y, \lambda, \varepsilon, m, j) = \theta_2(y^2 - 1) \quad (25)$$

Here, θ_2 is obtained by solving the nonlinear Equation (26).

$$2\theta_2(1 + j) + \lambda(1 - 0.75\theta_2\varepsilon)^m e^{\left(\frac{-0.75\theta_2}{1-0.75\theta_2\varepsilon}\right)} = 0 \quad (26)$$

The above nonlinear equation can be solved using wolframalpha.com for the given values of dimensionless parameters λ , j and ε .

Figure 3 compares the simulation results for the three geometries with the analytical expression. Based on the figure, the temperature in spherical geometries is assumed to be lower than in slabs.

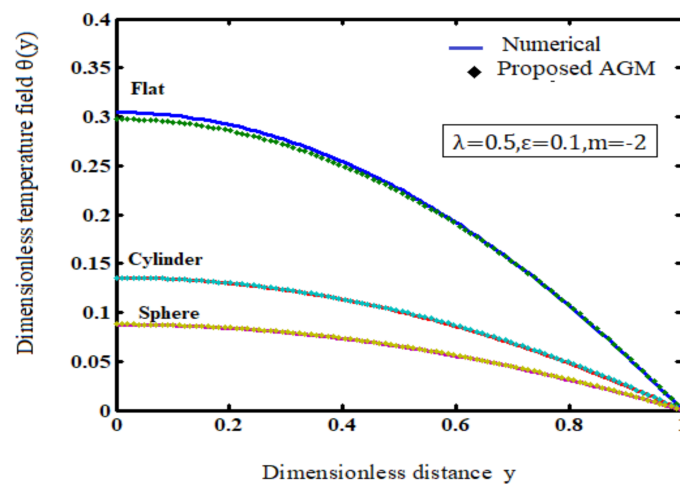


Figure 3. Comparison of analytical expression of temperature $\theta(y)$ (Equation (25)) with simulation results for flat $j = 0$, $\theta_2 = -0.29756$, cylinder $j = 1$, $\theta_2 = -0.135459$, and sphere $j = 2$, $\theta_2 = -0.0878074$.

8. Conclusions

We studied the exothermic explosion of a viscous combustible in slab, cylinder, and spherical geometries under Arrhenius, bimolecular, and sensitised laws of reaction schemes. The steady-state exothermic chemical reaction in a slab of combustible material was considered. We proved that this method provides an excellent approximation of the solution of this nonlinear system with high accuracy. The effects of the parameters of Frank-Kamenetskii number, the numerical exponent of temperature, and activation energy on temperature profiles are discussed.

Author Contributions: Conceptualization, M.E.G.L. and L.R.; methodology, M.E.G.L.; software, R.V.; validation, P.J.; formal analysis, L.R.; investigation, M.E.G.L.; resources, P.J.; data curation, P.J.; writing—original draft preparation, P.J.; writing—review and editing, P.J.; visualization, L.R.; supervision, M.E.G.L. and L.R.; project administration, M.E.G.L. All authors have read and agreed to the published version of the manuscript.

Funding: The authors have not received any funds.

Institutional Review Board Statement: Not applicable.

Informed Consent Statement: Not applicable.

Data Availability Statement: All raw numerical data are presented directly in text or as supplementary information.

Conflicts of Interest: The authors declare no conflict of interest.

Notations

a	Slab half width	m
A	Rate constant	None
C_0	Initial concentration of the reactant species	mol m ⁻³
E	Activation energy	kJ mol ⁻¹
h	Planck's number	Js
k	Thermal conductivity of the material	WmK ⁻¹
K	Boltzmann's constant	JK ⁻¹
Q	Heat of reaction	kJ mol
R	Universal gas constant	JK ⁻¹ mol ⁻¹
T	Absolute temperature	K
T_0	Wall temperature	K
ν	Vibration frequency	Hz
y	Dimensionless distance	None
Y	Distance measured in the normal direction in the plate	m
θ	Dimensionless temperature field	None
λ	Frank-Kamenetskii parameter	None
ε	Activation energy parameter	None
	The numerical exponent, such that	
m	$m = -2, 0, 1/2$ represent the numerical exponent for sensitised, Arrhenius, and bimolecular kinetics respectively.	None

Appendix A. Basic Concept of the Akbari–Ganji Method

Solving nonlinear differential equations is more challenging than solving linear differential equations. In this context, the Akbari–Ganji method (AGM) may be seen as a potent algebraic approach to resolving such issues. In the AGM, it is initially assumed that a solution function with unknown constant coefficients will satisfy both the initial conditions and the differential equation. Then, the unknown coefficients are calculated using algebraic equations established for IC and their derivatives. First, a polynomial is taken as the solution to the equation. The assumed constant coefficients of polynomials are then determined from the system of algebraic equations by solving the system of equations, which is then based on the boundary or initial conditions. The parameter y and its derivative are also a function of the nonlinear differential equation P . The parameter y itself is also a function of θ , and the order of the equation is m . The following are the steps of the AGM approach:

The given nonlinear equation can be expressed in the following way:

$$P_k : f\left(y, y', y'', \dots, y^{(m)}\right) = 0, \quad y = y(\theta) \quad (\text{A1})$$

where $k = 1$ to n . Boundary conditions from 0 to L are applied as follows:

$$\begin{cases} y(\theta) = y_0, y'(\theta) = y_1, \dots, y^{(m-1)}(\theta) = y_{m-1}, & \text{at } \theta = 0, \\ y(\theta) = y_{L_0}, y'(\theta) = y_{L_1}, \dots, y^{(m-1)}(\theta) = y_{L_{m-1}}, & \text{at } \theta = L. \end{cases} \quad (\text{A2})$$

In order to solve the differential equation, it is assumed that the solution to the differential equation is as follows:

$$y(\theta) = \sum_{i=0}^n \alpha_i y^i = \alpha_0 + \alpha_1 y + \alpha_2 y^2 + \dots + \alpha_n y^n. \quad (\text{A3})$$

The constant coefficients of the presumptive polynomial series are denoted by α_j . There are $n + 1$ unknown coefficients that need to be identified in order to solve the differential Equation (A1) using a series of order n equations. The following are the initial conditions (A2) that apply in Equation (A3). When $\theta = 0$, this becomes

$$\begin{cases} y(0) = y_0, \\ y'(0) = y_1, \\ y''(0) = \alpha_2 = y_2, \\ \dots \end{cases} \quad (\text{A4})$$

and when $\theta = L$, this can be written as follows:

$$\begin{cases} y(L) = \alpha_0 + \alpha_1 L + \alpha_2 L^2 + \dots + \alpha_n L^n = y_{L_0}, \\ y'(L) = \alpha_1 + 2\alpha_2 L + 3\alpha_3 L^2 + \dots + n\alpha_n L^{n-1} = y_{L_1}, \\ y''(L) = 2\alpha_2 + 6\alpha_3 L + 12\alpha_4 L^2 + \dots + n(n-1)\alpha_n L^{n-2} = y_{L_{n-1}}. \\ \dots \end{cases} \quad (\text{A5})$$

The following Equation (A6) is generated by substituting Equations (A4) and (A5) into Equation (A1):

$$\begin{aligned} P_0 &: f(y(0), y'(0), y''(0), \dots, y^{(m)}(0)) = 0, \\ P_1 &: f(y(L), y'(L), y''(L), \dots, y^{(m)}(L)) = 0 \end{aligned} \quad (\text{A6})$$

The series of order n is considered, and since ($n > m$), where m is the order of the differential equation, the number of equations is smaller than the number of unknowns. The Equation (A1) must be obtained, and the boundary values must be substituted in them to construct the $n + 1$ equations to calculate the $n + 1$ unknowns:

$$\begin{aligned} P'_k &: f(y', y'', y''', \dots, y^{(m-1)}) = 0, \\ P''_k &: f(y'', y''', y^{(IV)}, \dots, y^{(m+2)}) = 0. \end{aligned} \quad (\text{A7})$$

Once the system of equations is computed, the unknown coefficients $\alpha_0, \alpha_1, \dots, \alpha_n$ are calculated, and ultimately, the solution to the differential Equation (A1) is obtained.

References

- Hatchard, T.D.; MacNeil, D.D.; Basu, A.; Dahn, J.R. Thermal model of cylindrical and prismatic lithium-ion cells. *J. Electrochem. Soc.* **2001**, *148*, A755–A761. [[CrossRef](#)]
- Kim, G.H.; Pesaran, A.; Spotnitz, R. A three-dimensional thermal abuse model for lithium-ion cells. *J. Power Sources* **2007**, *170*, 476–489. [[CrossRef](#)]
- Peng, P.; Sun, Y.; Jiang, F. Thermal analyses of LiCoO₂ lithium-ion battery during oven tests. *Heat Mass Transf.* **2014**, *50*, 1405–1416. [[CrossRef](#)]
- Peng, P.; Sun, Y.; Jiang, F. Numerical simulations and thermal behavior analysis for oven thermal abusing of LiCoO₂ lithium-ion battery. *CIESC J.* **2014**, *65*, 647–657.
- Chiu, K.C.; Lin, C.H.; Yeh, S.F.; Lin, Y.H.; Chen, K.C. An electrochemical modeling of lithium-ion battery nail penetration. *J. Power Sources* **2014**, *251*, 254–263. [[CrossRef](#)]
- Wang, Q.; Ping, P.; Sun, J. Catastrophe analysis of cylindrical lithium ion battery. *Nonlinear Dyn.* **2010**, *61*, 763–772. [[CrossRef](#)]

7. Wang, Q.; Ping, P.; Zhao, X.; Chu, G.; Sun, J.; Chen, C. Thermal runaway caused fire and explosion of lithium ion battery. *J. Power Sources* **2012**, *208*, 210–224. [[CrossRef](#)]
8. Lisbona, D.; Snee, T. A review of hazards associated with lithium and lithium-ion batteries. *Process. Saf. Environ. Prot.* **2011**, *89*, 434–442. [[CrossRef](#)]
9. Ziebert, C.; Melcher, A.; Lei, B.; Zhao, W.; Rohde, M.; Seifert, H.J. Chapter Six—Electrochemical–Thermal Characterization and Thermal Modeling for Batteries. In *Emerging Nanotechnologies in Rechargeable Energy Storage Systems*; Micro and Nano Technologies: Karlsruhe Institute of Technology, Institute of Applied Materials—Applied Materials Physics: Eggenstein-Leopoldshafen, Germany, 2017; pp. 195–229.
10. Guo, G.; Long, B.; Cheng, B.; Zhou, S.; Cao, B. Three-dimensional thermal finite element modeling of lithium-ion battery in thermal abuse application. *J. Power Sources* **2010**, *195*, 2393–2398. [[CrossRef](#)]
11. Frank-Kamenetskii, D.A. *Diffusion and Heat Transfer in Chemical Kinetics*; Plenum Press: New York, NY, USA, 1969.
12. Boddington, T.; Gray, P.; Robinson, C. Thermal explosions and the disappearance of criticality at small activation energies: Exact results for the slab. *Proc. R. Soc. Lond.* **1979**, *368*, 441–461.
13. Boddington, T.; Feng, C.G.; Gray, P. Thermal explosions, criticality and the disappearance of criticality in systems with distributed temperatures. I. arbitrary biot number and general reaction rate laws. *Proc. R. Soc. Lond* **1983**, *390*, 247–264.
14. Boddington, T.; Gray, P.; Wake, G.C. Theory of thermal explosions with simultaneous parallel reactions. I. foundations and the one-dimensional case. *Proc. R. Soc. Lond.* **1984**, *393*, 85–100.
15. Graham-Eagle, J.G.; Wake, G.C. Theory of thermal explosions with simultaneous parallel reactions. II. The two- and three-dimensional cases and the variational method. *Proc. R. Soc. Lond. A* **1980**, *401*, 195–202.
16. Balakrishnan, E.; Swift, A.; Wake, G.C. Critical values for some nonclass A geometries in thermal ignition theory. *Math. Comput. Model.* **1996**, *24*, 1–10. [[CrossRef](#)]
17. Makinde, O.D. Exothermic explosions in a slab: A case study of series summation technique. *Int. Commun. Heat Mass Transf.* **2004**, *31*, 1227–1231. [[CrossRef](#)]
18. Ananthaswamy, V.; Subha, M. Analytical expressions for exothermic explosions in a slab. *Int. J. Res. Granthaalayah* **2014**, *1*, 22–33. [[CrossRef](#)]
19. Er-Riani, M.; Chetehouna, K. On the critical behaviour of exothermic explosions in class A geometries. *Math. Probl. Eng.* **2011**, *2011*, 536056. [[CrossRef](#)]
20. Heydari, H.; Avazzadeh, Z.; Cattan, C. Taylor’s series expansion method for nonlinear variable-order fractional 2D optimal control problems. *Alex. Eng. J.* **2020**, *59*, 4737–4743. [[CrossRef](#)]
21. He, J.H. Taylor series solution for a third order boundary value problem arising in Architectural Engineering. *Ain Shams Eng. J.* **2022**, *11*, 1411–1414. [[CrossRef](#)]
22. Wazwaz, A.-M. A reliable modification of Adomian decomposition method. *Appl. Math. Comput.* **1999**, *102*, 77–86. [[CrossRef](#)]
23. Abukhaled, M. Variational iteration method for nonlinear singular two-point boundary value problems arising in human physiology. *J. Math.* **2013**, *2013*, 720134. [[CrossRef](#)]
24. Dharmalingam, M.; Veeramuni, M. Akbari-Ganji’s method (AGM) for solving non-linear reaction—Diffusion equation in the electroactive polymer film. *J. Electroanal. Chem.* **2019**, *844*, 1–5. [[CrossRef](#)]
25. Meresht, N.B.; Ganji, D.D. Solving nonlinear differential equation arising in dynamical systems by AGM. *Int. J. Appl. Comput. Math.* **2017**, *3*, 1507–1523. [[CrossRef](#)]

Disclaimer/Publisher’s Note: The statements, opinions and data contained in all publications are solely those of the individual author(s) and contributor(s) and not of MDPI and/or the editor(s). MDPI and/or the editor(s) disclaim responsibility for any injury to people or property resulting from any ideas, methods, instructions or products referred to in the content.